Atmospheric
Chemistry
and Physics
Discussions

Open Access

A review of approaches to estimate wildfire plume injection height within large scale atmospheric chemical transport models – Part 1

R. Paugam[1], M. Wooster[1], S. R. Freitas[2], and M. Val Martin[3,4]

[1]King's College London, Environmental Monitoring and Modelling Research Group, Department of Geography, Strand, London, WC2R 2LS, UK
[2]Center for Weather Forecasting and Climate Studies, INPE, Cachoeira Paulista, Brazil
[3]Atmospheric Science Department, Colorado State University, Fort Collins, CO, USA
[4]Chemical and Biological Engineering Department, The University of Sheffield, Sheffield, UK

Correspondence to: R. Paugam (ronan.paugam@kcl.ac.uk)

ACPD

15, 9767–9813, 2015

Review on fire injection height – Part 1

R. Paugam et al.

Title Page

Abstract	Introduction
Conclusions	References
Tables	Figures

|◄　　►|

◄　　►

Back　Close

Full Screen / Esc

Printer-friendly Version

Interactive Discussion

Abstract

Landscape fires produce smoke containing a very wide variety of chemical species, both gases and aerosols. For larger, more intense fires that produce the greatest amounts of emissions per unit time, the smoke tends initially to be transported vertically or semi-vertically close by the source region, driven by the intense heat and convective energy released by the burning vegetation. The column of hot smoke rapidly entrains cooler ambient air, forming a rising plume within which the fire emissions are transported. This characteristics of this plume, and in particular the height to which it rises before releasing the majority of the smoke burden into the wider atmosphere, are important in terms of how the fire emissions are ultimately transported, since for example winds at different altitudes maybe quite different. This difference in atmospheric transport then may also affect the longevity, chemical conversion and fate of the plumes chemical consituents, with for example very high plume injection heights being associated with extreme long-range atmospheric transport. Here we review how such landscape-scale fire smoke plume injection heights are represented in larger scale atmospheric transport models aiming to represent the impacts of wildfire emissions on component of the Earth system. The use of satellite Earth observation (EO) data is commonly used for this, and detail the EO datasets capable of being used to remotely assess wildfire plume height distributions and the driving characteristics of the causal fires. We also discus both the physical mechanisms and dynamics taking place in fire plumes, and investigate the efficiency and limitations of currently available injection height parameterizations. Finally, we conclude by suggestion some future parameterization developments and ideas on EO data selection that maybe relevant to the instigation of enhanced methodologies aimed at injection height representation.

1 Introduction

Biomass burning is a major dynamic of the earth system (Bowman et al., 2009) responsible for the emission of massive quantities of trace gases and aerosols to the atmosphere (e.g. Andreae and Merlet, 2001; van der Werf et al., 2010). To understand and quantify the effects of these biomass burning emissions on atmospheric composition, air quality, weather, and climate, many fire emission inventories have been developed at scales ranging from individual areas, countries or regions (e.g. Sestak et al., 2002), continents (e.g. Turquety et al., 2007; Longo et al., 2010) or the entire global (e.g. FLAMBE, GFED, FINN, GFAS) (Reid et al., 2009; van der Werf et al., 2010; Wiedinmyer et al., 2011, respectively).

The use of satellite earth observation (EO) data are generally considered to be critical in providing the temporal coverage, spatial sampling frequency and directly observable parameters necessary for creating these inventories, particularly so since landscape fires are highly variable emissions sources, and the exact amounts of material released by the combustion process is highly variable in both space and time (Giglio et al., 2006; van der Werf et al., 2010; Kaiser et al., 2012).

When a landscape fire occurs, a rising plume created from the intense heat and convection produced by the energy released by burning vegetation interacts with the ambient atmosphere and transports the fire emissions, affecting their longevity, chemical conversion and fate (Freitas et al., 2006). This makes the manner in which the fire emissions are injected into the atmosphere highly variable, and sensitive to the smoke plume dynamics. For example, Fig. 1 shows EO satellite views of the evolution of the smoke plume generated by the "County Fire", which occurred in Ocala National Forest (Florida) in 2012. The fire was active from the 5 to the 13 of April 2012 and burned across nearly $14\,000\,\text{ha}$ ($140\,\text{km}^2$) of land. The apparent intensity and direction of travel of the smoke plume changes every day, and such variability is most likely related to both changes in the fire activity (for the former) and the local ambient atmospheric conditions (for the later). Together the fire and ambient atmospheric characteristics are the

main drivers of the plume dynamics, and therefore ultimately of the smoke emissions transport.

In addition to use of in-situ measurement (e.g. Johnson et al., 2008) and satellite earth observation (e.g. Wooster et al., 2012b), the wide ranging controls on and impacts of landscape scale fire emissions can be investigated using atmospheric chemistry transport models (CTMs) (e.g. Colarco et al., 2004; Turquety et al., 2007; Pfister et al., 2011). Such models require information on the quantity and timing of the fire emissions, as well as their chemical makeup, and these generally come from the aforementioned emissions inventories. However, for a more complete representation of the source fires, many CTMs can also make use of information on the altitude at which the bulk of the emitted species are injected into the wider atmosphere, where they can fully interact with ambient atmospheric circulation. Since at the typical resolution of CTMs we cannot resolve the plume dynamics, parameterizations are therefore required to represent these "smoke plume injection heights". The aim of this manuscript is to review the different approaches required for providing these parameterizations. The manuscript is structured as follows. First, Sect. 2 provides the background detail on fire plume observations and modelling in large scale CTMs. The main physical mechanisms responsible for the fire plume dynamics are discussed in Sect. 3. The primary satellite EO data used currently to study plume injection height properties are detailed in Sect. 4. Then, the currently available injection height models and their implementations are discussed in Sect. 5. Finally, a summary and suggestions for further developments in this area are provided in Sect. 6.

2 Introduction to landscape fire plume observations and modelling

Fire emissions are a particular case of emissions to the atmosphere, since they can be injected into the atmosphere far above the planetary boundary layer (PBL) and can thus potentially spread over long distance according to local atmospheric circulation patterns. Only emissions from aircraft traffic (Paugam et al., 2010) and volca-

noes (Woods, 1995), which are also coupled with intense dynamical mechanisms, offer a similar capability.

Injections of gases and aerosols emitted from vegetation fires have been observed at various heights in troposphere, and occasionally even the lower stratosphere (Fromm et al., 2005). Smoke remnants from certain tropical fires have been observed at 15 km altitude (Andreae et al., 2004), and plumes from individual Canadian stand-replacing forest fires can also reportedly approach such heights (Damoah et al., 2006). For the largest events, observations from Fromm et al. (2010) show that a single fire was able to induce a significant average surface temperature decrease at the hemispherical scale. The emissions from such large fire events are capable of spreading extremely rapidly, and Dirksen et al. (2009) show that the transport of emissions from an Australian fire in 2006 spread around the globe in only 12 days.

Using EO data from the Multi-angle Imaging SpectroRadiometer (MISR) instrument onboard the Terra satellite (Kahn et al., 2008) estimate that 5 to 18 % of 664 plumes observed from boreal forest fires over Alaska and the Canadian Yukon Territories in 2004 reached the free troposphere (FT). Using AI peak observation from TOMS, backward trajectories to identify location of the causal fire, and then GOES and/or American and Canadian fire reports data base for confirmation, Fromm et al. (2010) identify a total of 17 plumes that reached an altitude of at least 10 km for the year of 2002. Fires whose smoke columns reach these elevations are also likely to be those that emit large quantity of gases and aerosols, and therefore even if such large and intensely burning fires are relatively less common than smaller, less intense events, their impacts are likely to be much greater than the "average fire" (Chen et al., 2009). Actually, other evidence shows even smaller fire can generate plumes reaching the FT. Amiridis et al. (2010) show that half of the agricultural fires they observed over eastern Europe for the period 2006–2008 reach heights above the PBL. In summary, the height to which biomass burning plumes rise, and the distance over which the emissions are therefore transported, is highly variable. Possibly even more variable than fire behaviour, since the same fire burning under different ambient atmospheric conditions will probably result

in different plume behaviours. It is important to note however that certain atmospheric conditions are more favorable to fire occurrence than others, such as e.g. high pressure (Kahn et al., 2007) and/or low moisture (dry season) conditions (Labonne et al., 2007).

Fully modelling the impacts of biomass burning emissions at large scales requires an understanding of plume dynamics, including their injection height (InjH). Some InjH inventories are already available, for example derived from satellite EO data of aerosols or CO. For example,

– Guan et al. (2010) screened Aerosol Index (AI) measurements extracted from data collected by the Ozone Monitoring Instrument (OMI) and the Total Ozone Mapping Spectrometer (TOMS) to map high aerosol clouds ($> 5\,km$) related to wildfires, over the period 1978–2009;

– and (Gonzi and Palmer, 2010) use an inverse modelling method based on the GEOS-Chem model and EO-derived vertical measurements of CO concentration in the free troposphere and lower stratosphere (from the Tropospheric Emission Spectrometer (TES) and the Microwave Limb Sounder (MLS) sensors). The approach was able to retrieve an estimate of both the emitted CO magnitude and the injection height profile.

Although the above EO-based approaches are useful to understand and quantify the occurrence of wildfire plumes at different heights, they have limited sensitivity to the potential variability of InjH. Both inventories are therefore quite difficult to couple to fire emissions inventories, and cannot be easily linked to particular fires and therefore to actual emission totals. Capturing the high variability of plume dynamics, estimating injH, and implementing this within a CTM therefore remains a current topic of very active research (Freitas et al., 2010; Sofiev et al., 2012; Val Martin et al., 2012; Peterson et al., 2014), and the task of this manuscript is to review the different approaches currently available.

Title Page

Abstract | Introduction

Conclusions | References

Tables | Figures

|◄ | ►|

◄ | ►

Back | Close

Full Screen / Esc

Printer-friendly Version

Interactive Discussion

3 Physics of landscape fire plumes

The injection height of a smoke plume is controlled by the plume dynamics, which are driven by both the energy released by the fire and the ambient atmospheric conditions (both stability and humidity) (Kahn et al., 2007; Labonne et al., 2007). In the time period between the emissions being first released by the combustion process (which happens at the flame scale of $\sim$ mm), and their later release into the wider atmosphere (which operates on m to km scale), the smoke emissions are trapped in the plume (see Fig. 2). Here the dynamics are dominated by (i) the buoyancy flux induced by the Convective Heat Flux (CHF) generated by the fire itself, that is related to total heat released and so potentially to the Fire Radiative power (FRP) (Wooster et al., 2005; Freeborn et al., 2008), (ii) the size of the combustion zone, which controls the surface area of the plume interacting with the atmosphere (Freitas et al., 2007), (iii) the ambient atmospheric stratification (Kahn et al., 2008), (iv) the degree of turbulent mixing occurring at the edge of the plume, which affects the entrainment and detrainment of ambient air into the plume and which slows down the initial updraft and control the release of the smoke into the wider atmosphere (Kahn et al., 2007), (v) the wind shear, which also affects horizontal mixing and therefore the ent/detrainment mechanism in the plume, (vi) the latent heat released from the condensation of water vapour entrained into the plume from the combustion zone (water is a primary combustion product) and/or from the ambient fresh air (Freitas et al., 2007).

In some scenarios, the combination of these processes initially triggered by the heat released from the vegetation combustion is capable to producing deep convection in places where natural convection would not normally be possible; the so-called pyro-convection phenomena (Fromm et al., 2010). Trentmann et al. (2006) show that in the case of large events like the Chisholm fire (documented by Fromm and Servranckx, 2003), the energy budget of the plume is essentially driven by the latent heat released from the condensation of the entrained water vapour.

Depending on the quantity of water vapour condensed during the plumes development, three types of vegetation fire plume can be identified (Fromm et al., 2010):

i. Dry smoke plumes containing water vapour rather than liquid droplets. These are typically created by smaller, weakly burning and low intensity fires and usually stay trapped in the PBL.

ii. Pyro-Cumulus (PyroCu), which are formed from cloud droplets. Water vapour here condenses in the plume after it has reached the altitude of the Lifted-Condensation-Level (LCL). Depending of the stratification and ambient humidity of the atmosphere, these plumes maybe trapped in the PBL or reach the FT.

iii. Pyro-Cumulonimbus (PyroCb) which contain ice particles present in an anvil shape capped over the plume. Such plumes can reach the stratosphere, aided by the extra heat released from the ice formation. PyroCb are extreme cases and can be compared in nature to plumes from explosive volcanic eruptions. They are usually triggered by very large, intensely burning fires occurring in favorable atmospheric conditions for the phenomena. The exact conditions are still a matter of debate, however several studies have demonstrated the influence of fire size (Toon et al., 2006), unstable lower atmosphere (Kahn et al., 2007), and/or the presence of a cold front (Fromm et al., 2010; Dirksen et al., 2009; Luderer et al., 2006).

Of course, a full understanding of the complex coupled mechanisms inherent in fire plume dynamics is extremely challenging, and many points remain unclear. For example, the role of soot and aerosol in the heat transfer within the plume column (Trentmann et al., 2006) and the effect of the number of initial Cloud Condensation Nuclei (CCN) on the triggering of pyro-convection (Reutter et al., 2013).

Full Screen / Esc

Printer-friendly Version

Interactive Discussion

4 Earth observation data used to support wildfire injection height estimation

Sensors and imagers onboard EO satellites can provide various information on wild-fire plumes, including their trace gas ratios (e.g. Coheur et al., 2009; Ross et al., 2013), aerosol burden (e.g. Kaskaoutis et al., 2011; Ichoku and Ellison, 2014), and their height, including on occasion the vertical distribution of material within them (e.g. Kahn et al., 2008). Ichoku et al. (2012) provide a recent review of this topic. EO data also provide information on the characteristics of the causal fires themselves, including 'active fire' products that detail the location, timing and fire radiative power (FRP) of the landscape scale fires occurring within the EO satellite pixels (Giglio et al., 2003; Giglio and Schroeder, 2014; Peterson et al., 2014; Wooster et al., 2012a; Roberts and Wooster, 2008). FRP is a fire characteristic that has been shown to relate quite directly to the total heat produced by the combustion process (Freeborn et al., 2008), and also to the rate of fuel consumption (Wooster et al., 2005), trace gas (Freeborn et al., 2008) and aerosol (e.g. Ichoku et al., 2012) emission. Such active fire products are usually derived from thermal wavelength earth observations (Giglio et al., 2003; Roberts and Wooster, 2008; Wooster et al., 2012a).

No satellite product is yet able to derive information on plume heights at a spatial and temporal resolution than matches those of sensors used for active fire detection and smoke emission estimation, such as e.g. the Moderate Resolution Imaging Spectro-radiometer (MODIS), Meteosat SEVIRI, or the Geostationary Orbiting Environmental Satellite (GOES) (Giglio et al., 2003; Roberts and Wooster, 2008; Xu et al., 2010). Therefore, determination of the injection heights at spatio-temporal scales and levels of completeness approximately matching these type of active fire observations is more likely to rely on InjH parameterizations.

4.1 Direct measures of smoke plume height

Smoke plume height can be evaluated from space-borne plateform using either Lidar technology (Sect. 4.1.1) or stereo-matching algorithm based on passing imaging system (Sect. 4.1.2).

4.1.1 Spaceborne lidar

The primary spaceborne lidar used for estimating smoke plume heights is the Cloud-Aerosol Lidar and Infrared Pathfinder (CALIOP), operated onboard the Calipso satellite. CALIOP provides a backscatter signal at 562 and 1064 nm over a 70 m wide ground track. Measures in the two wavebands are used to derive a Level-2 product that classifies aerosol layers into dust, smoke, or marine classes, as well as providing height profiles (see Fig. 3). Calipso is part of the A-train satellite constellation, and flies 75 s behind the Aqua satellite. The main advantage provided by CALIOP is its high vertical resolution of 120 m, and its main limitations are (i) noise effects created by sunlight, that impact the results from daytime overpasses (Labonne et al., 2007) and (ii) the narrow ground track that limits the number of observed plumes that can be linked to their causal fires (Val Martin et al., 2010; Amiridis et al., 2010).

While the CALIOP level-2 product is able to directly sense the altitude and thickness of the plume layer detrained in the atmosphere (see Fig. 3 for a particular case where the plume axis is capture by the CALIOP track), most studies only refer to the top plume height, which in most case is used to determine the InjH measure (e.g. Val Martin et al., 2013).

Using CALIOP data, Labonne et al. (2007) examined plume heights from fires occurring in a number of countries and regions worldwide. Only in South Africa and Australian were definitive conclusions drawn, as in eastern Europe, Portugal, Indonesia and the western Unites States cloud cover was too complete and/or Calipso overpasses were not well timed with regard to regions affected by fires. Whilst Labonne et al. (2007) did not examine collocated CALIOP and active fire product data, they did

examine the bulk effect of fire emissions in South Africa and parts of Australia, where fire activity is mostly controlled by smaller, highly numerous savannah fires. They found that for most of the CALIOP ground track, the aerosol layer was trapped within the PBL. Their conclusion that most fires inject material into the PBL maybe true for this type of fire activity, but may not be the case for other regions such as forests where more intense fires can occur (Keeley, 2009). In another study based on CALIOP data covering eastern Europe, Amiridis et al. (2010) focused on agricultural fire emissions over 2006–2008. They found that 50 % of the 163 fires examined were above the PBL, with injection heights ranging from 1677 to 5940 m. Amiridis et al. (2010) collocated the CALIOP overpasses with MODIS active fire data from the Aqua satellite, and used fire radiative power (FRP) measures derived from the MODIS observations as a proxy for the strength of the fire activity. They concluded that the aerosols seen to be located above the PBL were a direct result of fire emissions, and were not related to large scale atmospheric transport. Furthermore, they demonstrated that in the presence of an unstable atmospheric layer in the troposphere a linear relationship holds between FRP (from MODIS) and plume-top height (from CALIOP). This is a similar result as that shown by Val Martin et al. (2010) with respect to MISR-derived plume heights (see below).

4.1.2 Stereo-imagers

Cloud-top heights have long been derived from stereo imaging, and the same methodology can be used to derive heights of smoke plumes (Mazzoni et al., 2007). The primary instrument used for this purpose is the Multi-angle Imaging SpectroRadiometer (MISR), operated aboard the NASA Terra satellite. This satellite is not part of the A-train, but rather has day time equator crossing of around 4 h before Aqua (at 10.30 a.m.). MISR can retrieve (i) total column aerosol optical thickness (AOT), and (ii) the altitude of the atmospheric cloud or aerosol layer over cloud-free land and water surfaces. The altitude retrieval is based on a stereo-matching algorithm that uses the 8 MISR collocated images available for each location wherever clouds or aerosol plumes

have discernible spatial contrast, with about 500 m vertical accuracy at a 1.1 km horizontal resolution (Kahn et al., 2007). The 380 km swath of MISR is centred within the 2330 km swath of the MODIS sensor present on the Terra satellite. Up to now, the specific derivation of smoke plume height from raw MISR data has been made using the MINX software tool (Nelson et al., 2013). Figure 4 shows an example of MINX output for a wildfire smoke plume, and Val Martin et al. (2010) provide full details of the use of MINX for this purpose. One constraint of MINX is the manual nature of the process required to digitize the smoke plume contour, used by the algorithm to compute the wind vector during the plume height retrieval. This wind vector is required to correct for the displacement occurring between the times of the 8 collocated but differently angled MISR views. Post processed plume heights for more than 25,000 plumes worldwide are accessible through the MISR Plume Height Project[1].

Because of its relatively high degree of spatial coverage Kahn et al. (2008) estimate that MISR is at a minimum 40 times more likely to observe a plume that can be linked to a causal fire than is CALIOP. Kahn et al. (2008) explain that MISR and CALIOP are, however, highly complementary since (i) they have different overpass local time as they are on differently orbiting satellites, and (ii) that CALIOP is able to detect optically thin older plumes, while MISR is essentially sensitive to only young plumes exhibiting high contrast with the background. One major drawback of MISR is, however, its relatively early daytime overpass, which limits its ability to observe mature PyroCu as they typically reach their maturity in the late afternoon (around 18:00 LT Fromm et al., 2010). Therefore, MISR-derived plume heights are biased toward lower altitude plumes (Val Martin et al., 2010). The relative lack of highly elevated plume observations from MISR was also reported by Chen et al. (2009). For some of the fire events encountered in their study, Chen et al. (2009) pointed out that the subsequent transport of CO and black carbon were better captured by a crude model of homogeneously spread emissions up to the top of the troposphere, than by an emission profile based on MISR-derived plume heights.

---

[1]http://www-misr.jpl.nasa.gov/getData/accessData/MisrMinxPlumes/

Statistical analyses of MISR-derived plume height data are available in Kahn et al. (2007), Mazzoni et al. (2007), Kahn et al. (2008), Val Martin et al. (2010), Tosca et al. (2011) and Jian and Fu (2014). These studies confirm that the majority of the detected plumes are trapped within the PBL, though geographical location and land cover type plan an influence. For example Kahn et al. (2008) show in their study on fires located in Alaska and the Yukon regions, that 5 to 18 % of the fires they observed for the summer 2004 reach the free troposphere, while Tosca et al. (2011) showed that the quasi totality of fires observed in Borneo and Sumatra (areas impacted strongly by peat fires) from 2001 to 2009 (317 fires) were trapped in the PBL. Val Martin et al. (2010) conducted a detailed analysis of the MISR-derived plume height data for fires in North America over a 5 years time period (2002, 2004–2007), finding no clear rules governing the capability of plumes to reach the FT, even when the fires were split per biome. However, Val Martin et al. (2010) show that the percentage of plumes reaching the FT in forest fires (more intense) was larger than crop/grassland fires (less intense).

The ATSR series of sensors have provided a 512 km wide swath stereo-viewing capability since 1991 (Prata et al., 1990), and recently Fisher et al. (2014) developed an automated stereo-height retrieval algorithm ($M6$) working with data from the advanced along-track scanning radiometer (AATSR). $M6$ was applied to AATSR data of Eurasian boreal forests for the period April-September of 4 years between 2008 to 2011, and showed successfull comparisons with collocated observations of smoke layer height derived from CALIOP lidar collections and MINX-derived stereo-heights from MISR. Unfortunately, AATSR also has a bias towards low injection heights since the overpass time is similar to MISR. A wider swath instrument following on from AATSR, the Sea and Land Surface Temperature Radiometer (SLSTR) will operate from 2015 (Wooster et al., 2012a). However, this will still not provide daily stereo-data worldwide, and with a limited number of stereo-observations the continuous, direct measurement of smoke plume heights at the global scale appears to be a difficult task.

4.2 Measure of buoyancy flux and fire size

Among the processes inherent to the plume dynamics and listed in Sect. 3, the buoyancy flux and the fire size are the two set of information needed to characterize the fire. The buoyancy flux generated by the combustion heat release is the primary source of energy responsible of the plume rise. The latent heat which provides energy to the plume is a secondary source which can be trigger only if the plume reaches LCL altitude. To understand the behaviour of the plume dynamics and explain variation in InjH, quantitative information on both the buoyant flux and the fire size are therefore needed. The vertical buoyant flux F is defined as (Viegas, 1998)

$$F = g\frac{(\rho - \rho_0)}{\rho}w = \frac{gR}{c_p p_0}Q_c, \tag{1}$$

where g is the gravity constant, R is the ideal gas constant, ρ is the density of the plume, w is the vertical velocity of the plume, ρ_0 and p_0 are the ambient density and pressure, c_p is the heat capacity at constant pressure and Q_c is the convective heat flux. According to experimental studies (mainly performed at small scale Freeborn et al., 2008; McCarter and Broido, 1965) fires tend to have constant partition of convective and radiative energy emission with a ratio β of convection to radiation ranging from 1 to 5, so that Q_c is related to the radiative heat flux Q_r, $Q_c = \beta Q_r$. In a model sensitivity study of the Chisholm fire run with the high resolution three-dimensional plume model ATHAM, Luderer et al. (2006) show that a ratio β greater than unity is crucial in their case to trigger the mechanism of pyro-convection. With value of β lower than unity, not enough latent heat is able to reach the condensation level.

A bi-spectral algorithm based on Middle Infra Red (MIR) and Thermal Infra Red (TIR) bands was proposed by Dozier (1981) to estimate the kinetic temperature T_f and the Active Fire (AF) area A_f of the black body that would emits the same radiances as the observed fire. According to the Stefan-Boltzmann equation $Q_r = \sigma T_f^4$ with σ the Boltzmann constant. This makes the buoyancy flux F a direct function of T_f. The Dozier

algorithm is therefore able to provide all information necessary to characterize the fire (i.e. $F = f(T_f)$ and fire size) as AF area can be used as a proxy for the fire size.

Several implementation of this algorithm have been developed and used with sensor of different resolution: e.g. the BIRD Hot spot Recognition Sensor (185 m Zhukov et al., 2006), MODIS (1 km Peterson et al., 2013), or GOES (3 km Prins et al., 1998). The algorithm is found to be highly sensitive to the determination of the long wave brightness temperature background (Giglio and Kendall, 2001), and in less respect to the atmospheric transmittance (Peterson and Wang, 2013). As a result it is not converging for $\approx 10\,\%$ of the case. However, this method represents the best option to estimate buoyancy flux and fire size.

5   Current representation of wildfire emissions injection height in CTMs

A number of studies have determined the very serious implications that incorrect InjH estimates have on the ability of CTMs to represent emissions transport (e.g. Hodzic et al., 2007; Turquety et al., 2007). Consequently it also have effects on: (i) "top-down" emission estimates based on the inversion of observed atmospheric concentrations of biomass burning species (Ichoku and Ellison, 2014) and (ii) radiative forcing studies (Ward et al., 2012). This section aims to review the different parameterizations that are currently available to tackle the issue of InjH. They are based either on empirical, deterministic, or statistical models.

5.1   Simple approaches: empirical and/or best-guessed profiles

Because of the complexity of fire plume dynamics, in the early endeavour of BB impact on the atmosphere, CTMs often assume a single fixed altitude for all biomass burning emissions usually presuming that all pollutants are contained solely within the PBL (e.g. Pfister et al., 2008; Hyer and Chew, 2010). However, such assumption cannot represent the observed variability of injection height described in Sect. 2. To improve

the representation of fire emission at large scale, some studies used a prescribed fixed profile either build on (i) simple hypothetical ratio between boundary layer and tropospheric emission (e.g. Turquety et al., 2007; Leung et al., 2007; Elguindi et al., 2010), or (ii) average local observations (Chen et al., 2009). In the later work, the author use the GEOS-Chem model with different vertical and temporal emissions distribution to simulate CO and aerosol transport over North America during the fire season 2004. Comparing their simulation results with satellite-, aircraft-, and ground-based measurements, they show that the use of finer temporal distribution enhances long term transport, while changes due to different InjH implementation are small. However, as already mentioned in Sect. 4.1, they also point out that the finer vertical modelled profile emission they implemented is probably affected by MISR observation bias. Most of these early studies do not provide grounded solutions to the problem of fire emission injection role in the atmospheric circulation but rather emphasis the challenge of developing InjH models.

5.2 Deterministic models

5.2.1 InjH models description

Several studies develop deterministic models capable of being host in CTM. They are usually based either on physical or dimensional analysis. Goodrick et al. (2013) review the different type of plume rise model existing. In particular, they discuss the use of plume rise model in the framework of the Blue Sky project, which aims to derive smoke emission system for air quality model such as CMAQ. Here, we restrain our review to plume rise models originally build to handle fire plume dynamics (see list of physical processes in Sect. 3). Models like Daysmoke (Achtemeier et al., 2011) or the Briggs equation (Briggs, 1975), which are both available in the CMAQ system, are more suitable for small fires like control burns (Achtemeier et al., 2011), to forecast or prevent emission dispersion and air pollution (i.e. local PM$_{2.5}$ concentration). When used with wildfires, they generally fail to predict large fire impact, certainly because of their weak

representation of micro physical processes (Achtemeier et al., 2011) which affect the simulation of PyroCu and PyroCb plumes. For example, using the Briggs equation and the CMAQ model to simulate fires emission in the US between 2006 and 2008, Raffuse et al. (2012) show that most of their plumes where below the level expected from remote-sensing measurement.

At present, three parameterizations of plume rise model stand out of the literature, namely: Freitas et al. (2007), Rio et al. (2010) and Sofiev et al. (2012). A brief description of each models is reported below.

– Freitas et al. (2007, 2010) develop a 1-dimension cloud resolving model (hereafter named Plume Rise Model version 0, PRMv0) based on the original plume model of Latham (1994), where equations for vertical momentum, first thermodynamic law and continuity of water phases are solved explicitly. The model is solved off-line and the final injection height is then used in the host CTM. In their approach the fire is modelled as an homogeneous circle defined with (i) a size derived form the Active Fire area of the WF-ABBA GOES product (Wild Fire Automated Biomass Burning Algorithm Prins et al., 1998) (ii) and a buoyant flux/CHF calculated as a constant fraction of the total heat. In their approach, the total heat is set as a prescribed value depending of the vegetation type. The cloud physics is based on a simple micro-physical module counting 3 hydrometeors (cloud, rain, ice). And the horizontal momentum is parametrized through two entrainment coefficients modelling the effect of (i) the turbulence at the edge of the stack ($\propto |w|/R$, Freitas et al., 2007) (ii) and the drag cause by the ambient wind shear ($\propto (u_e - u)/R$, Freitas et al., 2010). In previous formula, R is the radius of the plume, and u, u_e and w are the horizontal plume, horizontal ambient and vertical plume velocities. R, u, and w are prognostic variables of the model.

– Rio et al. (2010) implement in the LMDZ model a parameterization based on an Eddy Diffusivity/Mass Flux (EDMF) scheme originally developed to model similarly shallow convection and dry-convection. In comparison with the implementa-

Review on fire injection height – Part 1

R. Paugam et al.

Title Page

Abstract	Introduction
Conclusions	References
Tables	Figures

|◄   ►|

◄   ►

Back   Close

Full Screen / Esc

Printer-friendly Version

Interactive Discussion

tion of Freitas et al. (2007), this adaptation of EDMF for pyro-convection (pyro-EDMF hereafter) is not based on prognostic equation solved off-line, but rather evaluate turbulent flux produced by the temperature anomaly created by the fire at a sub-grid level and directly add the source term to the transport equations of the conservative variables of the host CTM. The fire is consider as a sub-grid effect and its CHF is modelled as a fraction of the host model mesh. The interest of this approach is that the dynamics of the plume is coupled with the ambient atmosphere, so that for example change in the stability of the atmosphere induced by the fire can impact the later development of the plume. In their approach, Rio et al. (2010) apply this extra turbulent flux to the total water, the liquid potential temperature and the CO_2 concentration, so that the effect of latent heat can be handle in the CTM, simplifying the formulation of the parameterization. Furthermore the mass flux formulation of Pyro-EDMF relies on the definition of both entrainment and detrainment fluxes which are set differently in the PBL and above. Therefore the mass transfer between the plume and the ambient atmosphere is solved all along the plume. One limitation of the current version of pyro-EDMF is the no representation of ambient shear at sub-grid level. This certainly over-predict injection height of small fires which are more sensible to wind drag.

– Sofiev et al. (2012) use energy balance in the up-draft and some dimensional analysis to develop an equation for the prediction of plume top height based on input of the FRP, the Brunt-Vaisala frequency and the PBL height. The equation parameters are fitted using a learning data set of plume height measurement randomly selected in the MISR data set. This formulation does not take explicitly into account effects from either entrainement, cloud formation or ambient wind shear. Another limitation of the equation of Sofiev et al. (2012) is inherent to the selection of the fires used to fit the equation parameters. All events from the learning (and the control) dataset used in this study are lower than 4 km. This implies that few PyroCu and certainly no PyroCb are present in the fit of the model.

5.2.2   InjH model validation: fire per fire comparison

Although validation on a fire per fire basis appears to be the best way to ensure the correct functioning of plume rise parameterization as when implemented in host model it is highly coupled with the large scale circulation, few validation exist and generally show poor agreement. In their original presentation, PRM and pyro-EDMF have been compared with documented fire events as for example the 3-D LES simulation of the Chisholm fire (Trentmann et al., 2006), but those tests (Freitas et al., 2010; Rio et al., 2010) are far from being a systematic validation ranging over different fire and atmosphere configuration. Example of those comparisons are reported in Figs. 5 and 6 for PRMv0 and pyro-EDMF, respectively.

Sessions et al. (2010) propose the first evaluation of the PRMv0 model. They run a comparison against ∼ 600 fires events captured by MISR that occur in Alaska in Spring 2008 during the 10 days of the NASA Arctic Research of the Composition of the Troposphere from Aircraft and Satellites (ARCTAS) campaign. They implement two fire initialization schemes both based on WF-ABBA and MODIS data for fire detection but using different temporal representation of the fire size based on either the diurnal cycle estimated in the FLAMBE inventory or kept constant as in the preprocessing of WRF-chem. They found the best comparison PRMv0-MISR for the FLAMBE based initialization with a one-to-one correlation of 0.45. They infer the bad response of PRMv0 partly to the quality of their atmospheric profile, emphasis the importance of correct atmospheric profile as already mentioned by Kahn et al. (2007).

More recently Val Martin et al. (2012) compare a subset of the MISR data set for North America with prediction from an improved version of PRMv0. Their model (PRMv1 hereafter) keeps the same model core, but uses a new initialization module where CHF and fire size information are derived for each fire from MODIS observation. Despite a selection of several method to estimate PRMv1 input data, Val Martin et al. (2012) show that over the large range of conditions encountered, PRMv1 is not able to reproduce the plume heights observed by MISR or to even locate the fire correctly

Review on fire injection height – Part 1

R. Paugam et al.

Title Page

Abstract	Introduction
Conclusions	References
Tables	Figures

Back | Close

Full Screen / Esc

Printer-friendly Version

Interactive Discussion

above or below the PBL. Their comparison is based on a total of 584 plumes selected from the MISR data where the following constraint apply: the plume height is computed immediately above the fire (not from the whole plume as in the original MISR data), the plume is formed of at least 5 stereo-height retrievals, the clustered MODIS fire pixels are located within 2 km of the plume origin, and the terrain height of the input atmospheric profile do not different from the terrain elevation used in the MINX software by more than 250 m. Despite this data quality screening, the best one-to-one correlation they obtain is about 0.3.

In their approach, Sofiev et al. (2012) use the whole MISR data set (counting 2000 fires at that time) without any filtering. Because of its derivation based on an optimization procedure, their model compares relatively well to the selected MISR data. However, when compared with the current full data set for North America, results are not as good, showing a constant underestimation of plume height, in particular for high plumes. Figure 7 shows together a comparison of our implementation of the Sofiev model against (i) the original version of the model, (ii) and against 3206 "good" quality flag fires of the North American subset of the MISR data set. Even if our implementation of the model exhibits a slight positive bias (certainly due to a different estimation of the PBL height which we read from the diagnostic products of the forecast run of ECMWF, 2012), our comparison with the MSIR data shows a strong negative bias of the model.

5.2.3   InjH models implementation

Despite the lack of conclusive fire per fire validation (see previous section), plume rise parameterizations have been implemented in several regional and large scale models. PRMv0 has been coupled with the The Weather Research and Forecasting (WRF) Model (Sessions et al., 2010; Grell et al., 2011; Pfister et al., 2011), the Coupled Aerosol and Tracer Transport model to the Brazilian developments on the Regional Atmospheric Modelling System (CATT-BRAMS Freitas et al., 2009; Longo et al., 2010) while pyro-EDMF is present in the Mesoscale Non Hydrostatic model (MesoNH Strada

Review on fire injection height – Part 1

R. Paugam et al.

Back | Close

Full Screen / Esc

Printer-friendly Version

Interactive Discussion

et al., 2012) and the general circulation model LMDZ (Rio et al., 2010) (see Table 1 of Val Martin et al., 2012, for a more complete list of models using plume rise parameterization).

Several studies highlight the need to inject fire emission at high altitude (Turquety et al., 2007; Elguindi et al., 2010), and recent in-situ (Cammas et al., 2009) and remote sensing (Fromm et al., 2010) observations show the frequent occurrence of large PyroCb. However, the role of plume-rise parameterization in transport of fire emission at large scale in CTM simulation is still a matter of debate. A list of different conclusion from recent studies is reported below.

- Sessions et al. (2010) who are using PRMv0 embedded in WRF-Chem, simulate 10 days of the Spring 2008 ARCTAS campaign. As for their fire-per-fire comparison (see previous section), they show that among their two initialization schemes, the used of the FLAMBE based initialization gives the best emission transport when compare with the Atmospheric InfraRed Sounder (AIRS) total columns CO and CALIOP aerosols profiles. Also a comparison with coarser injection schemes (distributing all fire emissions in the PBL or between altitude levels of 3 and 5 km) shows that the use of PRMv0 is improving the simulation.

- Rio et al. (2010) run simulations of the LMDZ model over the month of July 2006 for Africa on a strip located in the tropics between 5 and $20°$ S. Fires locations and emissions are estimated from the burnt area product L3JRC while fire activity is idealized with fire of constant size of $2\,km^2$ and a Gaussian diurnal cycle peaking at 15:45 LTC. Figure 8 show results from their simulations for different values of their parameter β which defines the ratio between entrainment and detrainment coefficients for levels above the PBL which are set as constant (no altitude dependence) and inversely proportional to the base of the plume radius. Their results show that pyro-EDMF is sensitive to value of the parameter β as detrainment altitude control the final spread of the emission. Rio et al. (2010) also show that LMDZ was more likely to predict the Daily Tropospheric Emission (DTE) of CO_2

Review on fire injection height – Part 1

R. Paugam et al.

Title Page

Abstract | Introduction

Conclusions | References

Tables | Figures

|◄ | ►|

◄ | ►

Back | Close

Full Screen / Esc

Printer-friendly Version

Interactive Discussion

(daily variation of CO_2 in the troposphere) observed by Chédin et al. (2005). However the simulated amplitude of DTE for southern Africa is still much lower than the observed value. Rio et al. (2010) focus only on tropical fire in Africa. In the tropics, natural convection is more active than in higher latitude and fire generated heat and vertical water transport could be a trigger to initiate natural convection (B. Johnson, private communication, 2013). Testing pyro-EDMF on boreal forest fire scenario would be interesting.

– Grell et al. (2011) run the WRF model coupled with PRMv0 initialized with fire size input data estimated from In-Situ measurement. Running WRF at cloud resolving scale over Alaska for 2 days for summer 2004, they show that the use of PRMv0 improve results comparison with radio sounding.

– Pfister et al. (2011) run WRF-Chem coupled with PRMv0 to examine CO budget in California over one month of the Summer 2008 coinciding with the ARCTAS campaign. WRF-Chem was also coupled with with the global Model for OZone and Related Chemical Tracers (MOZART) which is used to provide boundary condition. Such system allows the estimation of the relative importance of local sources versus pollution inflow on the distribution of CO at the surface and in the free troposphere. Fire emissions are based on the FINN inventory (Wiedinmyer et al., 2011) which in their case study shows a clear underestimation of CO emission over California. Model results are compared against airborne and ground measurement of CO as well CO total column from MOPITT. In the perspective of InjH modelling, Pfister et al. (2011) show that (i) in their case study PRMv0 injects half of the fire in the FT and captures well the timing and location of fire plume when compared with airborne CO measurements, (ii) and that their comparison with surfave measurement is impacted by a large underestimation of CO fire emission in the FINN inventory.

The conclusions of thoses studies emphasis the fact that the evaluation of plume rise effects on large scale atmospheric transport simulation is a challenging task. As emis-

Review on fire injection height – Part 1

R. Paugam et al.

Title Page

Abstract	Introduction
Conclusions	References
Tables	Figures

|◀ | ▶|

◀ | ▶

Back | Close

Full Screen / Esc

Printer-friendly Version

Interactive Discussion

sion transport is dependent form both quantity and the geographical location of the injection, to allow the evaluation of InjH estimation, both emission inventory and local condition (i.e. atmospheric profile) need to be correctly input.

5.3 Statistical models

As an alternative to the not reliable prediction of the PRM model, a statistically based approach using 584 plume height measures of the MISR dataset was presented by Val Martin et al. (2012). Classifying observed fires between low (< 1 km), medium (< 2.5 km), and high (> 2.5 km) plumes, they derive per biome the mean and standard deviation of FRP [MW] and atmospheric stable layer strength [$K\,km^{-1}$] for each plume height class (see Table 4 of Val Martin et al., 2012). Although this approach is attractive because of its inexpensive computational cost, its implementation appears to be difficult as most of the standard deviation for FRP and the stable layer strength are extremely high, yielding to cross-over between the characterisation of FRP and stable layer strength ranges of the different plume categories.

More recently Peterson et al. (2014) propose the idea of a model predicting the probability of injection above the PBL. Using an implementation of the Dozier (1981) algorithm based on MODIS input data, and 1028 boreal fire plumes extracted from the Northern American subset of the MISR dataset, they show that the presence of plume in the troposphere can be independently related to value of the classical FRP (Justice et al., 2002), fire size, FRP derived from the Dozier algorithm (FRP_f), or the FRP_f flux. Only showing trend between fire characteristic variation and probability of injection in the troposphere, no real model is formulated and their conclusion highlight the potential importance of atmospheric stability in the plume rise (which they did not take into account).

To our knowledge, no statistically based models has already been implemented in CTM. However, as their CPU cost would remain relatively low compare to any deterministic models, they show a great potential for implementation in large scale model,

in particular in climate model. However, their derivation is entirely relying on the good quality of their learning data set.

6   Summary and conclusions

Weakly burning landscape scale fires appear to release their smoke mainly into the planetary boundary layer, but larger and/or more intensely burning wildfires produce smoke columns that can rise rapidly and semi-vertically above the source region, driven by the intense heat and convective energy released by the burning vegetation. These columns of hot smoke entrains cooler ambient air, developing into a rising plume within which the trace gases and aerosols are transported to potentially quite high altitudes, in the most extreme cases into the stratosphere. The characteristics of these rising plumes, and in particular the height that they reach before releasing the majority of the smoke burden, is now acknowledged as an important control on the atmospheric transport of emissions from certain of these larger fire events (Colarco et al., 2004; Turquety et al., 2007; Rio et al., 2010). However, results comparing model-based estimates of smoke plume rise parameter to actual plume height observations made from satellite EO instruments (e.g. Ichoku et al., 2012) do not yet provide a strong quantitative agreement (Val Martin et al., 2012). Furthermore, the degree of improvement given by actually including plume rise parameterizations in atmosphere chemistry transport models can be difficult to interpret due to the complex interactions with other atmospheric processes Chen et al. (2009).

Apart from simulations based on single fire events, where plume injection height is carefully prescribed (Damoah et al., 2006; Dirksen et al., 2009), or where highly detailed simulations are run at very high resolution (Trentmann et al., 2006), the impact of fire induced up-draft on wildfire plume lofting appears, in general, to remain rather poorly understood and often weakly represented in current modelling efforts. The impact of possibly coupled effects to ambient atmospheric processes, such as the convection induced by the nearby presence of a cold front, are also not well determined.

At the scale of global CTMs, wildfire plume rise is generally represented by some form of parameterised model (Freitas et al., 2007; Rio et al., 2010; Sofiev et al., 2012). The ideal parameterization should solve the main physical processes responsible for the plume dynamics, using inputs regarding the fire characteristics that are available from EO satellites in near real time, and with concurrent measurements of fire activity and plume height from single fire events available to validate the resulting system (and reduce any impact from larger scale transport effects that influence comparisons of downwind plume characteristics).

Despite a demonstrated likely bias of MISR-derived plume heights towards lower plumes (Val Martin et al., 2010), the current MISR dataset for North America counts 22 fires with plume top higher that 4.5 km (see Figs. 9 and 10 for an overview of the current MISR data over North America). However, those high plumes might not be fully representative of standard fire behaviour as Fromm et al. (2010) show that PyroCu plume maturity peaks around 18:00 LT, and no fires are observed around that time with MISR (see bottom right plot of local time observation distribution in Fig. 10). Therefore, any PyroCu contained within the MISR-derived plume height dataset are certainly few in number, which leads to questions regarding the full representativeness of a random selection of fire events selected from this sample (Sofiev et al., 2012). In their approach Val Martin et al. (2012) apply several selection criteria when taking a subsample of fires extracted from the MISR plume height dataset for use in evaluation of their parameterised plume rise model, which is an adaptation of the widely used model of Freitas et al. (2007). However, even with this carefully selected evaluation dataset, the validation of this PRM model fails to show very convincing results. Nevertheless, in future, such validation (or optimization) of plume rise models should continue to pay attention to the quality of the evaluation datasets, including the following question:

i. Are the fire activity (FRP) and the plume dynamics (plume top height) linked? A time delay is necessary for the plume to dynamically adjust to change in the forcing induced by the energy release by the fire. For example, during the simulation of PyroCb of the Chisholm fire by the ATHAM model, it takes 40 min for

the plume to reach its stationary altitude with a constant forcing Trentmann et al. (2006). As the smoke plumes observed by MISR are more likely to in the relatively early stages of development due to the morning overpass of the Terra satellite (see Sect. 4.1.2), the effect of this time lag might be even more important than if fires were randomly observed at any time of their development.

ii. Is the radiation of the fire affecting by absorption from the plume. In low ambient wind conditions, the fire plume is often located just above the fire and in case of large fires this might mask some of the fire-emitted radiation due to the thick aerosol layer causing significant scattering and/or absorption of the radiant energy, possibly causing underestimation of FRP and unreliable CHF and fire size retrievals using the Dozier algorithm. As an example, we note that the fire from the MISR plume height data set observed with the highest plume height of 12 km (see bottom left plot of Fig. 10) is reported to have a relatively low total FRP of 6 GW (FRP of the strongest cluster in the vicinity of the plume), and a close inspection of the MODIS hot pixels shows that most of the fire pixels do not seem to be part of the plume dynamics (see Fig. 11). In this particularly extreme fire case, it seems that all fire pixels attached to the plume are located underneath it, and remain undetected by the MODIS active fire product.

Despite these difficulties, the range of relevant data provided on actively burning fires and their smoke plumes by EO satellites continues to grow (e.g. Ichoku et al., 2012), and these improving capabilities, together with continuing advances in the extent to which plume rise models can be parameterised and incorporated into large-scale atmospheric chemistry transport models (Peterson et al., 2014; Paugam et al., 2015), can be expected to continue to advance the accuracy of smoke plume injection estimates and the resulting impact on long-range atmospheric transport of these globally important emissions.

References

Achtemeier, G. L., Goodrick, S. A., Liu, Y., Garcia-Menendez, F., Hu, Y., and Odman, M. T.: Modeling smoke plume-rise and dispersion from Southern United States prescribed burns with daysmoke, Atmosphere, 2, 358–388, doi:10.3390/atmos2030358, 2011. 9782, 9783

Amiridis, V., Giannakaki, E., Balis, D. S., Gerasopoulos, E., Pytharoulis, I., Zanis, P., Kazadzis, S., Melas, D., and Zerefos, C.: Smoke injection heights from agricultural burning in Eastern Europe as seen by CALIPSO, Atmos. Chem. Phys., 10, 11567–11576, doi:10.5194/acp-10-11567-2010, 2010. 9771, 9776, 9777

Andreae, M. O. and Merlet, P.: Emission of trace gases and aerosols from biomass burning, Global Biogeochem. Cy., 15, 955–966, doi:10.1029/2000GB001382, 2001. 9769

Andreae, M. O., Rosenfeld, D., Artaxo, P., Costa, A. A., Frank, G. P., Longo, K. M., and Silva-Dias, M. A. F.: Smoking rain clouds over the Amazon, Science, 303, 1337–1342, doi:10.1126/science.1092779, 2004. 9771

Bowman, D. M. J. S., Balch, J. K., Artaxo, P., Bond, W. J., Carlson, J. M., Cochrane, M. A., D'Antonio, C. M., DeFries, R. S., Doyle, J. C., Harrison, S. P., Johnston, F. H., Keeley, J. E., Krawchuk, M. A., Kull, C. A., Marston, J. B., Moritz, M. A., Prentice, I. C., Roos, C. I., Scott, A. C., Swetnam, T. W., van der Werf, G. R., and Pyne, S. J.: Fire in the Earth system, Science, 324, 481–484, doi:10.1126/science.1163886, 2009. 9769

Briggs, G. A.: Plume rise equations, in: Lectures on Air Pollution and Environmental Impact Analyses, edited by: Haugen, D., AMS, Boston, MA, USA, 59–111, 1975. 9782

Cammas, J.-P., Brioude, J., Chaboureau, J.-P., Duron, J., Mari, C., Mascart, P., Nédélec, P., Smit, H., Pätz, H.-W., Volz-Thomas, A., Stohl, A., and Fromm, M.: Injection in the lower stratosphere of biomass fire emissions followed by long-range transport: a MOZAIC case study, Atmos. Chem. Phys., 9, 5829–5846, doi:10.5194/acp-9-5829-2009, 2009. 9787

Chédin, A., Serrar, S., Scott, N. A., Pierangelo, C., and Ciais, P.: Impact of tropical biomass burning emissions on the diurnal cycle of upper tropospheric CO_2 retrieved from NOAA 10 satellite observations, J. Geophys. Res.-Atmos., 110, doi:10.1029/2004JD005540, 2005. 9788

Chen, Y., Li, Q., Randerson, J. T., Lyons, E. A., Kahn, R. A., Nelson, D. L., and Diner, D. J.: The sensitivity of CO and aerosol transport to the temporal and vertical distribution of North American boreal fire emissions, Atmos. Chem. Phys., 9, 6559–6580, doi:10.5194/acp-9-6559-2009, 2009. 9771, 9778, 9782, 9790

5 Coheur, P.-F., Clarisse, L., Turquety, S., Hurtmans, D., and Clerbaux, C.: IASI measurements of reactive trace species in biomass burning plumes, Atmos. Chem. Phys., 9, 5655–5667, doi:10.5194/acp-9-5655-2009, 2009. 9775

Colarco, P. R., Schoeberl, M. R., Doddridge, B. G., Marufu, L. T., Torres, O., and Welton, E. J.: Transport of smoke from Canadian forest fires to the surface near Washington, D.C.: injection height, entrainment, and optical properties, J. Geophys. Res.-Atmos., 109, n/a–n/a, doi:10.1029/2003JD004248, 2004. 9770, 9790

Damoah, R., Spichtinger, N., Servranckx, R., Fromm, M., Eloranta, E. W., Razenkov, I. A., James, P., Shulski, M., Forster, C., and Stohl, A.: A case study of pyro-convection using transport model and remote sensing data, Atmos. Chem. Phys., 6, 173–185, doi:10.5194/acp-6-173-2006, 2006. 9771, 9790

15 Dirksen, R. J., Folkert Boersma, K., de Laat, J., Stammes, P., van der Werf, G. R., Val Martin, M., and Kelder, H. M.: An aerosol boomerang: Rapid around-the-world transport of smoke from the December 2006 Australian forest fires observed from space, J. Geophys. Res.-Atmos., 114, D21201, doi:10.1029/2009JD012360, 2009. 9771, 9774, 9790

20 Dozier, J.: A method for satellite identification of surface temperature fields of subpixel resolution, Remote Sens. Environ., 11, 221–229, doi:10.1016/0034-4257(81)90021-3, 1981. 9780, 9789

ECMWF: IFS documentation Part IV: Physical Processes, Tech. Rep. CY38r1, European Center for Medium-Range Weather Forecasts, Shinfield Park, Reading, UK, available at: http://old.ecmwf.int/research/ifsdocs/CY38r1/IFSPart4.pdf (last access: March 2015), 2012. 9786, 9809

Elguindi, N., Clark, H., Ordóñez, C., Thouret, V., Flemming, J., Stein, O., Huijnen, V., Moinat, P., Inness, A., Peuch, V.-H., Stohl, A., Turquety, S., Athier, G., Cammas, J.-P., and Schultz, M.: Current status of the ability of the GEMS/MACC models to reproduce the tropospheric CO vertical distribution as measured by MOZAIC, Geosci. Model Dev., 3, 501–518, doi:10.5194/gmd-3-501-2010, 2010. 9782, 9787

Fisher, D., Muller, J.-P., and Yershov, V.: Automated stereo retrieval of smoke plume injection heights and retrieval of smoke plume masks from AATSR and their as-

Title Page

Abstract | Introduction

Conclusions | References

Tables | Figures

|◄ | ►|

◄ | ►

Back | Close

Full Screen / Esc

Printer-friendly Version

Interactive Discussion

sessment with CALIPSO and MISR, IEEE T. Geosci. Remote, 52, 1249–1258, doi:10.1109/TGRS.2013.2249073, 2014. 9779

Freeborn, P. H., Wooster, M. J., Hao, W. M., Ryan, C. A., Nordgren, B. L., Baker, S. P., and Ichoku, C.: Relationships between energy release, fuel mass loss, and trace gas and aerosol emissions during laboratory biomass fires, J. Geophys. Res.-Atmos., 113, D01301, doi:10.1029/2007JD008679, 2008. 9773, 9775, 9780

Freitas, S. R., Longo, K. M., and Andreae, M. O.: Impact of including the plume rise of vegetation fires in numerical simulations of associated atmospheric pollutants, Geophys. Res. Lett., 33, L17808, doi:10.1029/2006gl026608, 2006. 9769

Freitas, S. R., Longo, K. M., Chatfield, R., Latham, D., Silva Dias, M. A. F., Andreae, M. O., Prins, E., Santos, J. C., Gielow, R., and Carvalho Jr., J. A.: Including the sub-grid scale plume rise of vegetation fires in low resolution atmospheric transport models, Atmos. Chem. Phys., 7, 3385–3398, doi:10.5194/acp-7-3385-2007, 2007. 9773, 9783, 9784, 9791, 9807

Freitas, S. R., Longo, K. M., Silva Dias, M. A. F., Chatfield, R., Silva Dias, P., Artaxo, P., Andreae, M. O., Grell, G., Rodrigues, L. F., Fazenda, A., and Panetta, J.: The Coupled Aerosol and Tracer Transport model to the Brazilian developments on the Regional Atmospheric Modeling System (CATT-BRAMS) – Part 1: Model description and evaluation, Atmos. Chem. Phys., 9, 2843–2861, doi:10.5194/acp-9-2843-2009, 2009. 9786

Freitas, S. R., Longo, K. M., Trentmann, J., and Latham, D.: Technical Note: Sensitivity of 1-D smoke plume rise models to the inclusion of environmental wind drag, Atmos. Chem. Phys., 10, 585–594, doi:10.5194/acp-10-585-2010, 2010. 9772, 9783, 9785, 9807

Fromm, M., Bevilacqua, R., Servranckx, R., Rosen, J., Thayer, J. P., Herman, J., and Larko, D.: Pyro-cumulonimbus injection of smoke to the stratosphere: observations and impact of a super blowup in northwestern Canada on 3–4 August 1998, J. Geophys. Res.-Atmos., 110, D08205, doi:10.1029/2004JD005350, 2005. 9771

Fromm, M., Lindsey, D. T., Servranckx, R., Yue, G., Trickl, T., Sica, R., Doucet, P., and Godin-Beekmann, S.: The untold story of Pyrocumulonimbus, B. Am. Meteorol. Soc., 91, 1193–1209, doi:10.1175/2010BAMS3004.1, 2010. 9771, 9773, 9774, 9778, 9787, 9791

Fromm, M. D. and Servranckx, R.: Transport of forest fire smoke above the tropopause by supercell convection, Geophys. Res. Lett., 30, 1542, doi:10.1029/2002GL016820, 2003. 9773

Giglio, L. and Kendall, J. D.: Application of the Dozier retrieval to wildfire characterization: a sensitivity analysis, Remote Sens. Environ., 77, 34–49, doi:10.1016/S0034-4257(01)00192-4, 2001. 9781

Title Page

Abstract | Introduction

Conclusions | References

Tables | Figures

|◄ | ►|

◄ | ►

Back | Close

Full Screen / Esc

Printer-friendly Version

Interactive Discussion

Giglio, L. and Schroeder, W.: A global feasibility assessment of the bi-spectral fire temperature and area retrieval using {MODIS} data, Remote Sens. Environ., 152, 166–173, doi:10.1016/j.rse.2014.06.010, 2014. 9775

Giglio, L., Descloitres, J., Justice, C. O., and Kaufman, Y. J.: An enhanced contextual fire detection algorithm for {MODIS}, Remote Sens. Environ., 87, 273–282, doi:10.1016/S0034-4257(03)00184-6, 2003. 9775, 9803, 9813

Giglio, L., Csiszar, I., and Justice, C. O.: Global distribution and seasonality of active fires as observed with the Terra and Aqua Moderate Resolution Imaging Spectroradiometer (MODIS) sensors, J. Geophys. Res., 111, G02016, doi:10.1029/2005jg000142, 2006. 9769

Gonzi, S. and Palmer, P. I.: Vertical transport of surface fire emissions observed from space, J. Geophys. Res.-Atmos., 115, D02306, doi:10.1029/2009JD012053, 2010. 9772

Goodrick, S. L., Achtemeier, G. L., Larkin, N. K., Liu, Y., and Strand, T. M.: Modelling smoke transport from wildland fires: a review, Int. J. Wildland Fire, 22, 83–94, 2013. 9782

Grell, G., Freitas, S. R., Stuefer, M., and Fast, J.: Inclusion of biomass burning in WRF-Chem: impact of wildfires on weather forecasts, Atmos. Chem. Phys., 11, 5289–5303, doi:10.5194/acp-11-5289-2011, 2011. 9786, 9788

Guan, H., Esswein, R., Lopez, J., Bergstrom, R., Warnock, A., Follette-Cook, M., Fromm, M., and Iraci, L. T.: A multi-decadal history of biomass burning plume heights identified using aerosol index measurements, Atmos. Chem. Phys., 10, 6461–6469, doi:10.5194/acp-10-6461-2010, 2010. 9772

Hodzic, A., Madronich, S., Bohn, B., Massie, S., Menut, L., and Wiedinmyer, C.: Wildfire particulate matter in Europe during summer 2003: meso-scale modeling of smoke emissions, transport and radiative effects, Atmos. Chem. Phys., 7, 4043–4064, doi:10.5194/acp-7-4043-2007, 2007. 9781

Hyer, E. J. and Chew, B. N.: Aerosol transport model evaluation of an extreme smoke episode in Southeast Asia, Atmos. Environ., 44, 1422–1427, doi:10.1016/j.atmosenv.2010.01.043, 2010. 9781

Ichoku, C. and Ellison, L.: Global top-down smoke-aerosol emissions estimation using satellite fire radiative power measurements, Atmos. Chem. Phys., 14, 6643–6667, doi:10.5194/acp-14-6643-2014, 2014. 9775, 9781

Ichoku, C., Kahn, R., and Chin, M.: Satellite contributions to the quantitative characterization of biomass burning for climate modeling, Atmos. Res., 111, 1–28, doi:10.1016/j.atmosres.2012.03.007, 2012. 9775, 9790, 9792

Title Page

Abstract | Introduction

Conclusions | References

Tables | Figures

◀ | ▶

◀ | ▶

Back | Close

Full Screen / Esc

Printer-friendly Version

Interactive Discussion

Jian, Y. and Fu, T.-M.: Injection heights of springtime biomass-burning plumes over peninsular Southeast Asia and their impacts on long-range pollutant transport, Atmos. Chem. Phys., 14, 3977–3989, doi:10.5194/acp-14-3977-2014, 2014. 9779

Johnson, B. T., Osborne, S. R., Haywood, J. M., and Harrison, M. A. J.: Aircraft measurements of biomass burning aerosol over West Africa during DABEX, J. Geophys. Res.-Atmos., 113, D00C06, doi:10.1029/2007JD009451, 2008. 9770

Justice, C., Giglio, L., Korontzi, S., Owens, J., Morisette, J., Roy, D., Descloitres, J., Alleaume, S., Petitcolin, F., and Kaufman, Y.: The {MODIS} fire products, Remote Sens. Environ., 83, 244–262, doi:10.1016/S0034-4257(02)00076-7, the Moderate Resolution Imaging Spectro-radiometer (MODIS): a new generation of Land Surface Monitoring, 2002. 9789

Kahn, R. A., Li, W.-H., Moroney, C., Diner, D. J., Martonchik, J. V., and Fishbein, E.: Aerosol source plume physical characteristics from space-based multiangle imaging, J. Geophys. Res.-Atmos., 112, D11205, doi:10.1029/2006JD007647, 2007. 9772, 9773, 9774, 9778, 9779, 9785

Kahn, R. A., Chen, Y., Nelson, D. L., Leung, F.-Y., Li, Q., Diner, D. J., and Logan, J. A.: Wildfire smoke injection heights: two perspectives from space, Geophys. Res. Lett., 35, L04809, doi:10.1029/2007GL032165, 2008. 9771, 9773, 9775, 9778, 9779

Kaiser, J. W., Heil, A., Andreae, M. O., Benedetti, A., Chubarova, N., Jones, L., Morcrette, J.-J., Razinger, M., Schultz, M. G., Suttie, M., and van der Werf, G. R.: Biomass burning emissions estimated with a global fire assimilation system based on observed fire radiative power, Biogeosciences, 9, 527–554, doi:10.5194/bg-9-527-2012, 2012. 9769

Kaskaoutis, D., Kharol, S. K., Sifakis, N., Nastos, P., Sharma, A. R., Badarinath, K., and Kambezidis, H.: Satellite monitoring of the biomass-burning aerosols during the wild-fires of August 2007 in Greece: climate implications, Atmos. Environ., 45, 716–726, doi:10.1016/j.atmosenv.2010.09.043, 2011. 9775

Keeley, J. E.: Fire intensity, fire severity and burn severity: a brief review and suggested usage, Int. J. Wildland Fire, 18, 116, doi:10.1071/wf07049, 2009. 9777

Labonne, M., Bréon, F.-M., and Chevallier, F.: Injection height of biomass burning aerosols as seen from a spaceborne lidar, Geophys. Res. Lett., 34, L11806, doi:10.1029/2007GL029311, 2007. 9772, 9773, 9776

Latham, D.: PLUMP: A one-dimensional plume predictor and cloud model for fire and smoke managers, General Technical Report INT-GTR-314, Intermountain Research Station, USDA Forest Service, November, 1994. 9783

Leung, F.-Y. T., Logan, J. A., Park, R., Hyer, E., Kasischke, E., Streets, D., and Yurganov, L.: Impacts of enhanced biomass burning in the boreal forests in 1998 on tropospheric chemistry and the sensitivity of model results to the injection height of emissions, J. Geophys. Res.-Atmos., 112, D10313, doi:10.1029/2006JD008132, 2007. 9782

Longo, K. M., Freitas, S. R., Andreae, M. O., Setzer, A., Prins, E., and Artaxo, P.: The Coupled Aerosol and Tracer Transport model to the Brazilian developments on the Regional Atmospheric Modeling System (CATT-BRAMS) – Part 2: Model sensitivity to the biomass burning inventories, Atmos. Chem. Phys., 10, 5785–5795, doi:10.5194/acp-10-5785-2010, 2010. 9769, 9786

Luderer, G., Trentmann, J., Winterrath, T., Textor, C., Herzog, M., Graf, H. F., and Andreae, M. O.: Modeling of biomass smoke injection into the lower stratosphere by a large forest fire (Part II): sensitivity studies, Atmos. Chem. Phys., 6, 5261–5277, doi:10.5194/acp-6-5261-2006, 2006. 9774, 9780

Mazzoni, D., Logan, J. A., Diner, D., Kahn, R., Tong, L., and Li, Q.: A data-mining approach to associating {MISR} smoke plume heights with {MODIS} fire measurements, Remote Sens. Environ., 107, 138–148, doi:10.1016/j.rse.2006.08.014, 2007. 9777, 9779

McCarter, R. J. and Broido, A.: Radiative and convective energy from wood crib fires, Pyrodynamics, 2, 65–85, 1965. 9780

Nelson, D. L., Chen, Y., Kahn, R. A., Diner, D. J., and Mazzoni, D.: Example applications of the MISR INteractive eXplorer (MINX) software tool to wildfire smoke plume analyses, Proc. SPIE, 7089, 708909–708911, doi:10.1117/12.795087, 2008. 9806, 9809, 9811, 9812, 9813

Nelson, D. L., Garay, M. J., Kahn, R. A., and Dunst, B. A.: Stereoscopic height and wind retrievals for aerosol plumes with the MISR INteractive eXplorer (MINX), Remote Sens., 5, 4593–4628, doi:10.3390/rs5094593, 2013. 9778

Paugam, R., Paoli, R., and Cariolle, D.: Influence of vortex dynamics and atmospheric turbulence on the early evolution of a contrail, Atmos. Chem. Phys., 10, 3933–3952, doi:10.5194/acp-10-3933-2010, 2010. 9770

Paugam, R., Wooster, M., Atherton, J., Freitas, S. R., Schultz, M. G., and Kaiser, J. W.: Development and optimization of a wildfire plume rise model based on remote sensing data inputs – Part 2, Atmos. Chem. Phys. Discuss., 15, 9815–9895, doi:10.5194/acpd-15-9815-2015, 2015. 9792

Peterson, D. and Wang, J.: A sub-pixel-based calculation of fire radiative power from {MODIS} observations: 2. sensitivity analysis and potential fire weather application, Remote Sens. Environ., 129, 231–249, doi:10.1016/j.rse.2012.10.020, 2013. 9781

Peterson, D., Wang, J., Ichoku, C., Hyer, E., and Ambrosia, V.: A sub-pixel-based calculation of fire radiative power from {MODIS} observations: 1: algorithm development and initial assessment, Remote Sens. Environ., 129, 262–279, doi:10.1016/j.rse.2012.10.036, 2013. 9781

Peterson, D., Hyer, E., and Wang, J.: Quantifying the potential for high-altitude smoke injection in the North American boreal forest using the standard MODIS fire products and subpixel-based methods, J. Geophys. Res.-Atmos., 119, 3401–3419, doi:10.1002/2013JD021067, 2014. 9772, 9775, 9789, 9792

Pfister, G. G., Wiedinmyer, C., and Emmons, L. K.: Impacts of the fall 2007 California wildfires on surface ozone: integrating local observations with global model simulations, Geophys. Res. Lett., 35, L19814, doi:10.1029/2008GL034747, 2008. 9781

Pfister, G. G., Avise, J., Wiedinmyer, C., Edwards, D. P., Emmons, L. K., Diskin, G. D., Podolske, J., and Wisthaler, A.: CO source contribution analysis for California during ARCTAS-CARB, Atmos. Chem. Phys., 11, 7515–7532, doi:10.5194/acp-11-7515-2011, 2011. 9770, 9786, 9788

Prata, A., Cechet, R., Barton, I., and Llewellyn-Jones, D.: The along track scanning radiometer for ERS-1-scan geometry and data simulation, IEEE T. Geosci. Remote, 28, 3–13, doi:10.1109/36.45741, 1990. 9779

Prins, E. M., Feltz, J. M., Menzel, W. P., and Ward, D. E.: An overview of GOES-8 diurnal fire and smoke results for SCAR-B and 1995 fire season in South America, J. Geophys. Res.-Atmos., 103, 31821–31835, doi:10.1029/98JD01720, 1998. 9781, 9783

Raffuse, S. M., Craig, K. J., Larkin, N. K., Strand, T. T., Sullivan, D. C., Wheeler, N. J. M., and Solomon, R.: An evaluation of modeled plume injection height with satellite-derived observed plume height, Atmosphere, 3, 103–123, doi:10.3390/atmos3010103, 2012. 9783, 9805

Reid, J., Hyer, E., Prins, E., Westphal, D., Zhang, J., Wang, J., Christopher, S., Curtis, C., Schmidt, C., Eleuterio, D., Richardson, K., and Hoffman, J.: Global monitoring and forecasting of biomass-burning smoke: description of and lessons from the fire locating and modeling of burning emissions (FLAMBE) program, IEEE J. Sel. Top. Appl., 2, 144–162, doi:10.1109/JSTARS.2009.2027443, 2009. 9769

Reutter, P., Trentmann, J., Seifert, A., Neis, P., Su, H., Chang, D., Herzog, M., Wernli, H., Andreae, M. O., and Pöschl, U.: 3-D model simulations of dynamical and microphysical inter-

Title Page

Abstract | Introduction

Conclusions | References

Tables | Figures

|◄ | ►|

◄ | ►

Back | Close

Full Screen / Esc

Printer-friendly Version

Interactive Discussion

actions in pyroconvective clouds under idealized conditions, Atmos. Chem. Phys., 14, 7573–7583, doi:10.5194/acp-14-7573-2014, 2014. 9774

Rio, C., Hourdin, F., and Chédin, A.: Numerical simulation of tropospheric injection of biomass burning products by pyro-thermal plumes, Atmos. Chem. Phys., 10, 3463–3478, doi:10.5194/acp-10-3463-2010, 2010. 9783, 9784, 9785, 9787, 9788, 9790, 9791, 9808, 9810

Roberts, G. and Wooster, M.: Fire detection and fire characterization over Africa using Meteosat SEVIRI, IEEE T. Geosci. Remote, 46, 1200–1218, doi:10.1109/tgrs.2008.915751, 2008. 9775

Ross, A. N., Wooster, M. J., Boesch, H., and Parker, R.: First satellite measurements of carbon dioxide and methane emission ratios in wildfire plumes, Geophys. Res. Lett., 40, 4098–4102, doi:10.1002/grl.50733, 2013. 9775

Sessions, W. R., Fuelberg, H. E., Kahn, R. A., and Winker, D. M.: An investigation of methods for injecting emissions from boreal wildfires using WRF-Chem during ARCTAS, Atmos. Chem. Phys. Discuss., 10, 26551–26606, doi:10.5194/acpd-10-26551-2010, 2010. 9785, 9786, 9787

Sestak, M., O'Neill, S., Ferguson, S., Ching, J., and Fox, D.: Integration of Wildfire Emissions into Models-3/Cmaq with the Prototypes: Community Smoke Emissions Modeling System (CSEM) and BLUESKY, Models-3 User's Workshop, October 21–23, EPA, Research Triangle Park, NC, USA, 2002. 9769

Sofiev, M., Ermakova, T., and Vankevich, R.: Evaluation of the smoke-injection height from wildland fires using remote-sensing data, Atmos. Chem. Phys., 12, 1995–2006, doi:10.5194/acp-12-1995-2012, 2012. 9772, 9783, 9784, 9786, 9791, 9809

Strada, S., Mari, C., Filippi, J.-B., and Bosseur, F.: Wildfire and the atmosphere: modelling the chemical and dynamic interactions at the regional scale, Atmos Environ., 51, 234–249, doi:10.1016/j.atmosenv.2012.01.023, 2012. 9786

Toon, O. B., Turco, R. P., Robock, A., Bardeen, C., Oman, L., and Stenchikov, G. L.: Atmospheric effects and societal consequences of regional scale nuclear conflicts and acts of individual nuclear terrorism, Atmos. Chem. Phys. Discuss., 6, 11745–11816, doi:10.5194/acpd-6-11745-2006, 2006. 9774

Tosca, M. G., Randerson, J. T., Zender, C. S., Nelson, D. L., Diner, D. J., and Logan, J. A.: Dynamics of fire plumes and smoke clouds associated with peat and deforestation fires in Indonesia, J. Geophys. Res.-Atmos., 116, D08207, doi:10.1029/2010JD015148, 2011. 9779

Title Page

Abstract | Introduction

Conclusions | References

Tables | Figures

|◀ | ▶|

◀ | ▶

Back | Close

Full Screen / Esc

Printer-friendly Version

Interactive Discussion

Trentmann, J., Luderer, G., Winterrath, T., Fromm, M. D., Servranckx, R., Textor, C., Herzog, M., Graf, H.-F., and Andreae, M. O.: Modeling of biomass smoke injection into the lower stratosphere by a large forest fire, Part I: reference simulation, Atmos. Chem. Phys. Discuss., 6, 6041–6080, doi:10.5194/acpd-6-6041-2006, 2006. 9773, 9774, 9785, 9790, 9792, 9807

5 Turquety, S., Logan, J. A., Jacob, D. J., Hudman, R. C., Leung, F. Y., Heald, C. L., Yantosca, R. M., Wu, S., Emmons, L. K., Edwards, D. P., and Sachse, G. W.: Inventory of boreal fire emissions for North America in 2004: importance of peat burning and pyroconvective injection, J. Geophys. Res.-Atmos., 112, D12S03, doi:10.1029/2006JD007281, 2007. 9769, 9770, 9781, 9782, 9787, 9790

10 Val Martin, M., Logan, J. A., Kahn, R. A., Leung, F.-Y., Nelson, D. L., and Diner, D. J.: Smoke injection heights from fires in North America: analysis of 5 years of satellite observations, Atmos. Chem. Phys., 10, 1491–1510, doi:10.5194/acp-10-1491-2010, 2010. 9776, 9777, 9778, 9779, 9791

Val Martin, M., Kahn, R. A., Logan, J. A., Paugam, R., Wooster, M., and Ichoku, C.: Space-
15 based observational constraints for 1-D fire smoke plume-rise models, J. Geophys. Res.-Atmos., 117, D22204, doi:10.1029/2012JD018370, 2012. 9772, 9785, 9787, 9789, 9790, 9791

Val Martin, M., Heald, C. L., Ford, B., Prenni, A. J., and Wiedinmyer, C.: A decadal satellite analysis of the origins and impacts of smoke in Colorado, Atmos. Chem. Phys., 13, 7429–
20 7439, doi:10.5194/acp-13-7429-2013, 2013. 9776

van der Werf, G. R., Randerson, J. T., Giglio, L., Collatz, G. J., Mu, M., Kasibhatla, P. S., Morton, D. C., DeFries, R. S., Jin, Y., and van Leeuwen, T. T.: Global fire emissions and the contribution of deforestation, savanna, forest, agricultural, and peat fires (1997–2009), Atmos. Chem. Phys., 10, 11707–11735, doi:10.5194/acp-10-11707-2010, 2010. 9769, 9811

25 Viegas, D. X.: Convective processes in forest fires, in: Buoyant Convection in Geophysical Flows, Kluwer Academic Publishers, AA Dordrecht, the Netherlands, 401–420, 1998. 9780

Ward, D. S., Kloster, S., Mahowald, N. M., Rogers, B. M., Randerson, J. T., and Hess, P. G.: The changing radiative forcing of fires: global model estimates for past, present and future, Atmos. Chem. Phys., 12, 10857–10886, doi:10.5194/acp-12-10857-2012, 2012. 9781

30 Wiedinmyer, C., Akagi, S. K., Yokelson, R. J., Emmons, L. K., Al-Saadi, J. A., Orlando, J. J., and Soja, A. J.: The Fire INventory from NCAR (FINN): a high resolution global model to estimate the emissions from open burning, Geosci. Model Dev., 4, 625–641, doi:10.5194/gmd-4-625-2011, 2011. 9769, 9788

Woods, A. W.: The dynamics of explosive volcanic eruptions, Rev. Geophys., 33, 495–530, doi:10.1029/95RG02096, 1995. 9771

Wooster, M. J., Roberts, G., Perry, G. L. W., and Kaufman, Y. J.: Retrieval of biomass combustion rates and totals from fire radiative power observations: FRP derivation and calibration relationships between biomass consumption and fire radiative energy release, J. Geophys. Res.-Atmos., 110, D24311, doi:10.1029/2005JD006318, 2005. 9773, 9775

Wooster, M., Xu, W., and Nightingale, T.: Sentinel-3 SLSTR active fire detection and FRP product: pre-launch algorithm development and performance evaluation using MODIS and ASTER datasets, Remote Sens. Environ., 120, 236–254, doi:10.1016/j.rse.2011.09.033, 2012a. 9775, 9779

Wooster, M. J., Perry, G. L. W., and Zoumas, A.: Fire, drought and El Niño relationships on Borneo (Southeast Asia) in the pre-MODIS era (1980–2000), Biogeosciences, 9, 317–340, doi:10.5194/bg-9-317-2012, 2012b. 9770

Xu, W., Wooster, M., Roberts, G., and Freeborn, P.: New GOES imager algorithms for cloud and active fire detection and fire radiative power assessment across North, South and Central America, Remote Sens. Environ., 114, 1876–1895, doi:10.1016/j.rse.2010.03.012, 2010. 9775

Zhukov, B., Lorenz, E., Oertel, D., Wooster, M., and Roberts, G.: Spaceborne detection and characterization of fires during the bi-spectral infrared detection (BIRD) experimental small satellite mission (2001–2004), Remote Sens. Environ., 100, 29–51, doi:10.1016/j.rse.2005.09.019, 2006. 9781
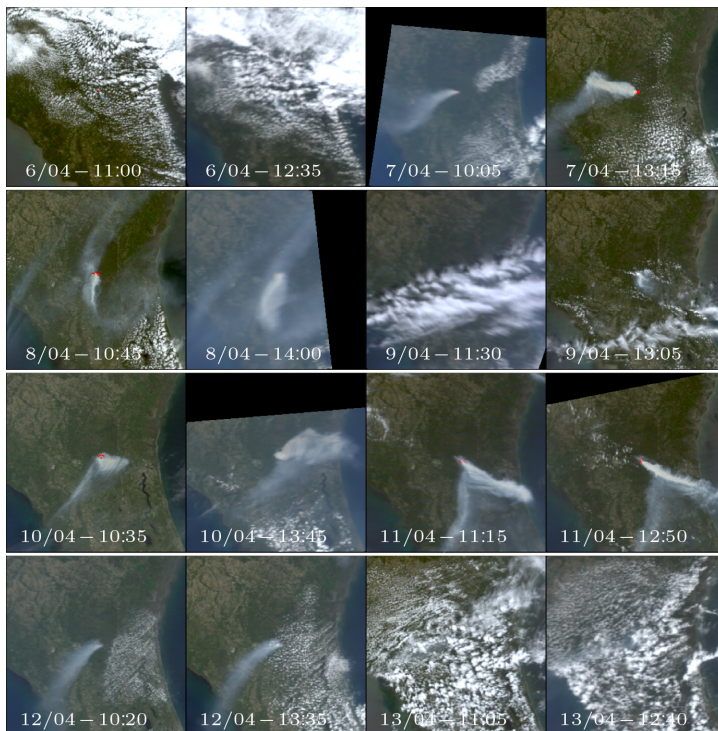
Figure 1. True colour composite of daytime observations of the County fire (US), made from the Moderate Resolution Imaging Spectroradiometer (MODIS) satellite EO sensor. The fire occurred in Ocala National Forest (Florida) between 5 and 13 April 2012. MODIS data from all available Terra and Aqua satellite overpasses are shown, with the local time indicated. Overlain on the colour composite imagery are red vectors that outline pixels detected as containing active fires by the MODIS MOD14/MYD14 Active Fire and Thermal Anomaly Products (Giglio et al., 2003). The regularly changing nature of the fire and the smoke transport apparent from this time series, as well as the presence on some days of bifurcated plumes, is very apparent.
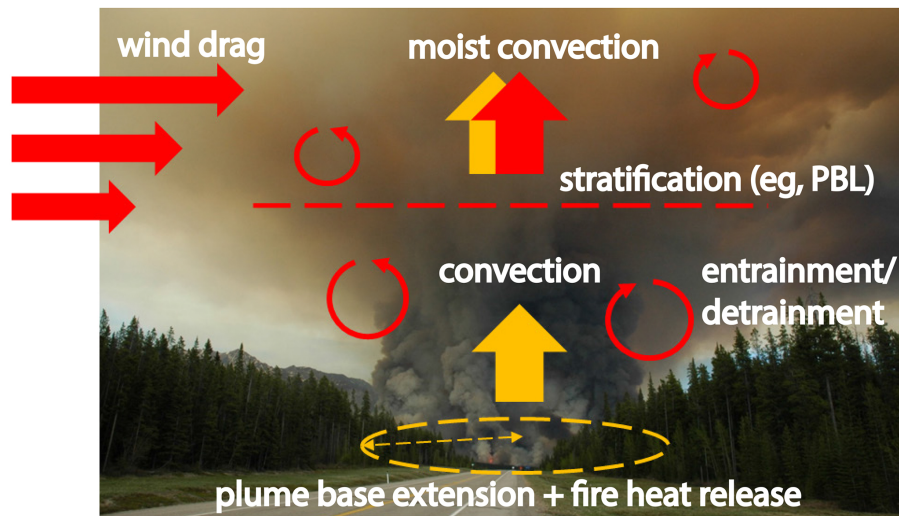
Figure 2. Schematic view of the physical processes involved in fire plume dynamics. Red and yellow colours stand for atmospheric or fire induced mechanisms respectively.
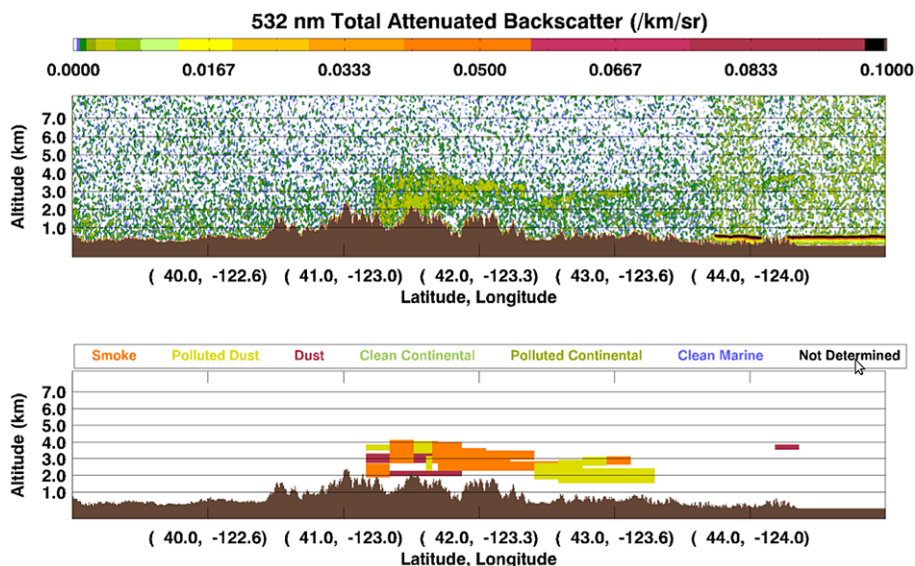
Figure 3. Example of profiles for Level-1 CALIOP 532 nm total attenuated backscatter data product (top), and the matching level-2 product of aerosol layers (bottom) for the 28 August 2006 over the Klamath mountains in California and Oregon. The presence of aerosols classified as biomass burning smoke can be seen. Image from Raffuse et al. (2012).
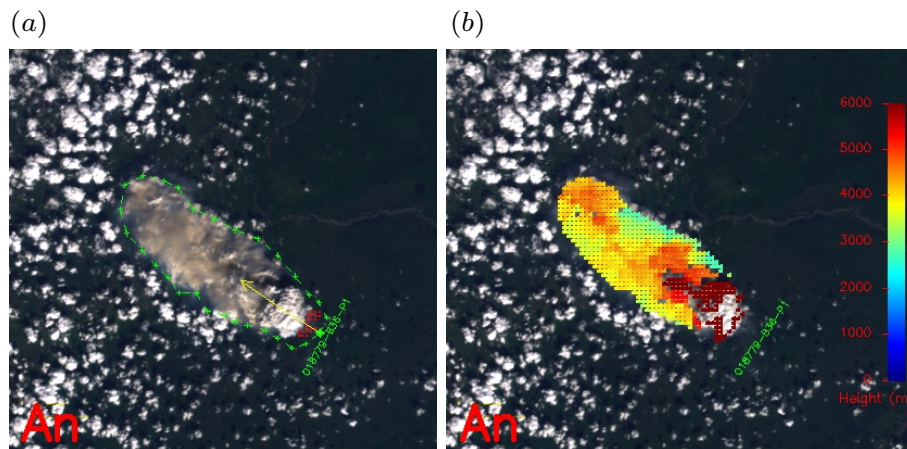
Figure 4. Example of smoke plume height derivation using data from the Multiangle Imaging SpectroRadiometer (MISR) that operates on the Terra satellite. The fire took place on the 29 June 2003 in Alaska, and was observed by MISR at 21:41 UTC and is referenced in the MISR data set as 018779-B36-P1. The user-defined smoke plume contour shown in **(a)** is used by the MINX software (Nelson et al., 2008) to derive the plume stereo-heights shown in **(b)**. Background images are the MISR nadir views, and the locations of MODIS-derived active fire pixels are shown in red on **(b)**. Image taken from the MISR plume height project website (see Footnote 1).
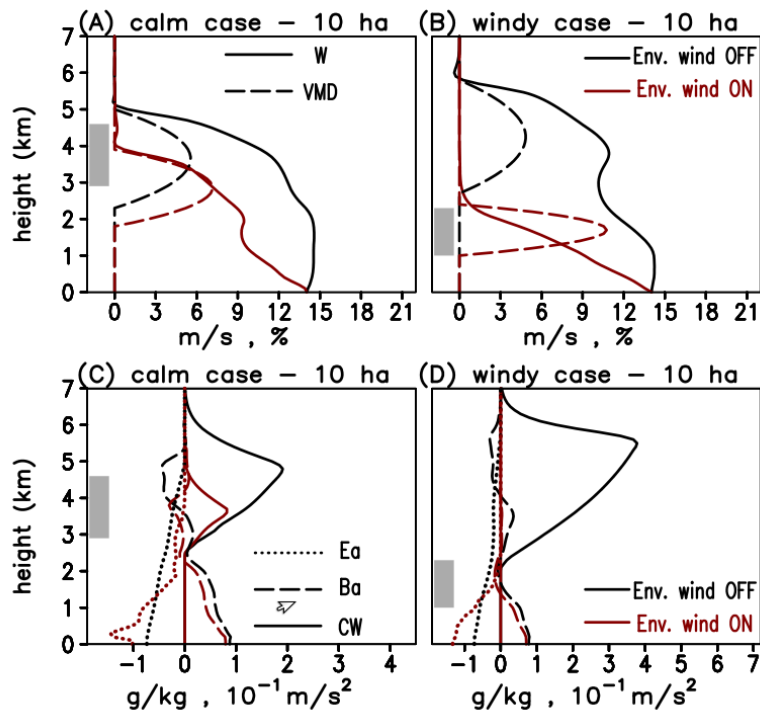
Figure 5. Results from the 1-D plume rise model (PRM) of Freitas et al. (2007, 2010) for a fire burning in **(a, c)** calm and **(b, d)** windy atmosphere scenario, as studied by Freitas et al. (2010). The fire has an active fire area (AF-area) of 10 ha. The quantities shown are: vertical velocity (W, $m\,s^{-1}$), vertical mass distribution (VMD, %), entrainment acceleration (Ea, $10^{-1}\,m\,s^{-2}$), buoyancy acceleration (Ba, $10^{-1}\,m\,s^{-2}$), and total condensate water (CW, $g\,kg^{-1}$). Model results considering the environmental wind drag are shown in red, whilst those in black depicts the results from simulations disregarding this effect. Grey rectangles indicate the main injection height simulated by the 3-D ATHAM model (Trentmann et al., 2006) for the same fire scenario. Figure from Freitas et al. (2010).

Title Page

Abstract | Introduction

Conclusions | References

Tables | Figures

|◄ | ►|

◄ | ►

Back | Close

Full Screen / Esc

Printer-friendly Version
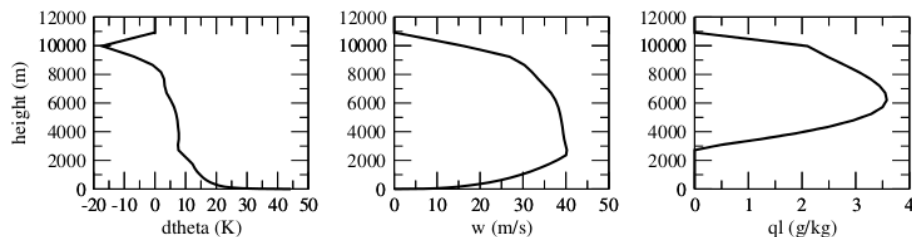
Interactive Discussion

Figure 6. Smoke plume characteristics for the Chisholm fire, as simulated by pyro-EDMF: virtual potential temperature (K), vertical velocity excess ($\mathrm{m\,s^{-1}}$),and cloud liquid water ($\mathrm{g\,kg^{-1}}$) are shown. Figure from Rio et al. (2010).

Title Page

Abstract | Introduction

Conclusions | References

Tables | Figures

|◄ | ►|

◄ | ►

Back | Close

Full Screen / Esc

Printer-friendly Version
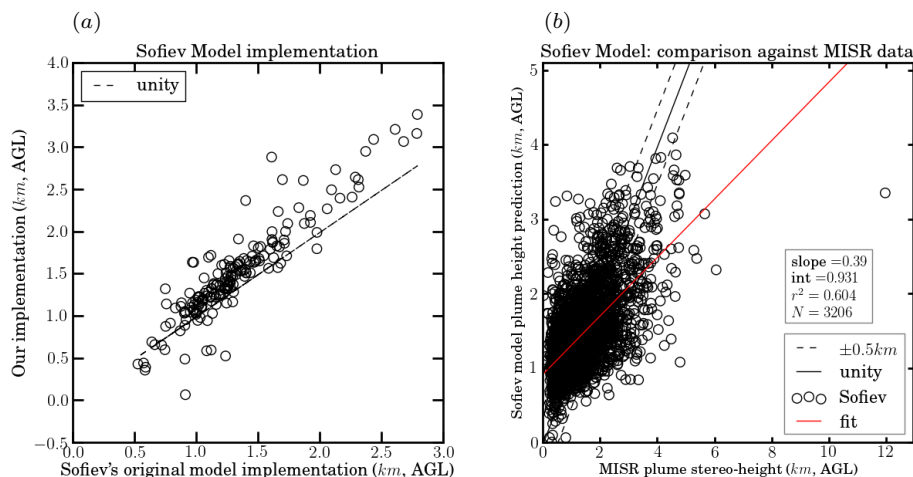
Interactive Discussion

Figure 7. Comparison of our implementation of the plume rise parameterisation of Sofiev et al. (2012) to **(a)** the original results from Sofiev et al. (2012) for the same fires, and **(b)** plume stereo-height retrievals extracted from the North-American subset of the (MISR) plume height project data Nelson et al. (2008), derived using the MINX tool as shown in Fig. 4. Our implementation of the Sofiev et al. (2012) model differs from the original in its definition of the PBL height, which in our approach is extracted from the diagnostic product of ECMWF forecast runs (ECMWF, 2012). See Figs. 9 and 10 for a statistical overview of the Northern American MISR data set. Note that the Sofiev et al. (2012) model did not retrieve simulated plume heights for all the 3320 selected fires of that dataset. For 114 fires, either the Brunt-Vaisala frequency could not be retrieved or the FRP of the most powerful pixel listed in the MISR product were unavailable (see Sofiev et al., 2012, for details in the initialisation of the model).
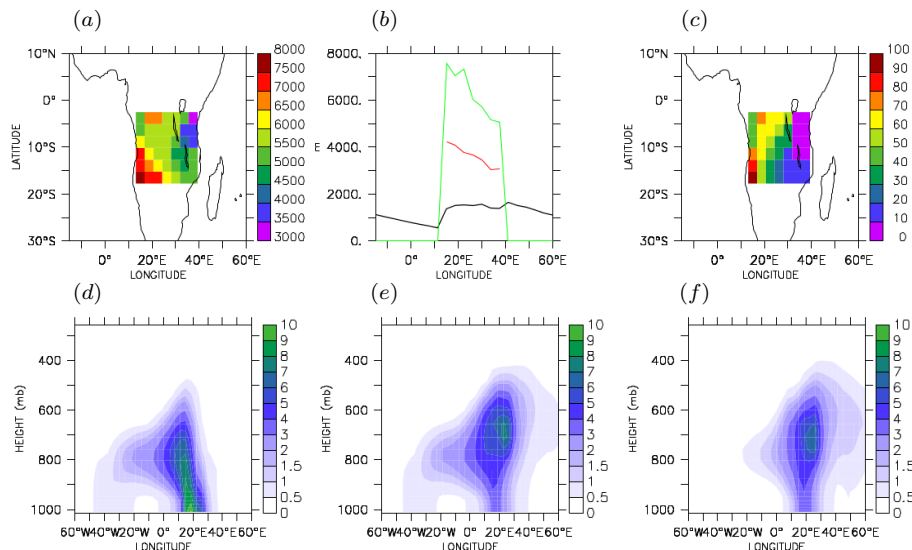
Figure 8. Simulations performed using the pyro-EDMF plume rise model of Rio et al. (2010) for sub-Saharan Africa between 10 and 30 July 2006. In the upper panel **(a)** shows the maximal Injection height of CO_2 emissions simulated with the LMDZ model and pyro-EDMF between 5 and 20° S over the 20 days of the simulation. **(b)** reports the maximal injection height (green), mean injection height of emissions injected above the boundary layer height (red), and mean boundary layer height (black) averaged between 5 and 20° S altitude and over the 20 days of the simulation. **(c)** shows the percentage of cases for which the injection height passing the boundary layer height. In lower panel **(e)** shows the averaged vertical distribution of CO_2 mixing ratio (ppmv) for the same reference simulation and **(d)** for simulations without pyro-EDMF, and **(f)** with pyro-EDMF set up with a lower value of the ratio β = entrainment/detrainment = 0.1 (right). The reference simulation in **(e)** uses a value of β = 0.4. Figure from Rio et al. (2010).

Title Page

Abstract | Introduction

Conclusions | References

Tables | Figures

|◀ | ▶|

◀ | ▶

Back | Close

Full Screen / Esc

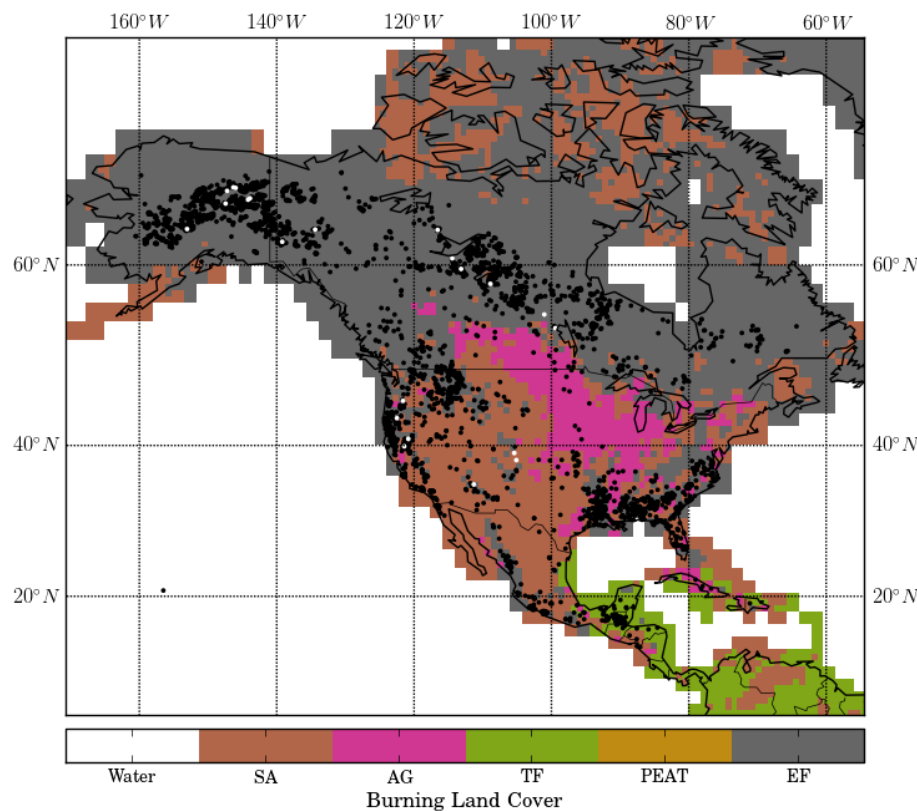Printer-friendly Version

Interactive Discussion

Figure 9. Fire locations contained within the Multi-angle Imaging Spectro Radiometer (MISR) plume height dataset of (Nelson et al., 2008) over North America for the time period 2001–2008 (black dots). The map in the background shows the land cover used within the GFEDv3 biomass burning emissions inventory of van der Werf et al. (2010). White dots indicate the locations of the 22 fires plumes classed as having a plume height in excess of 4.5 km.
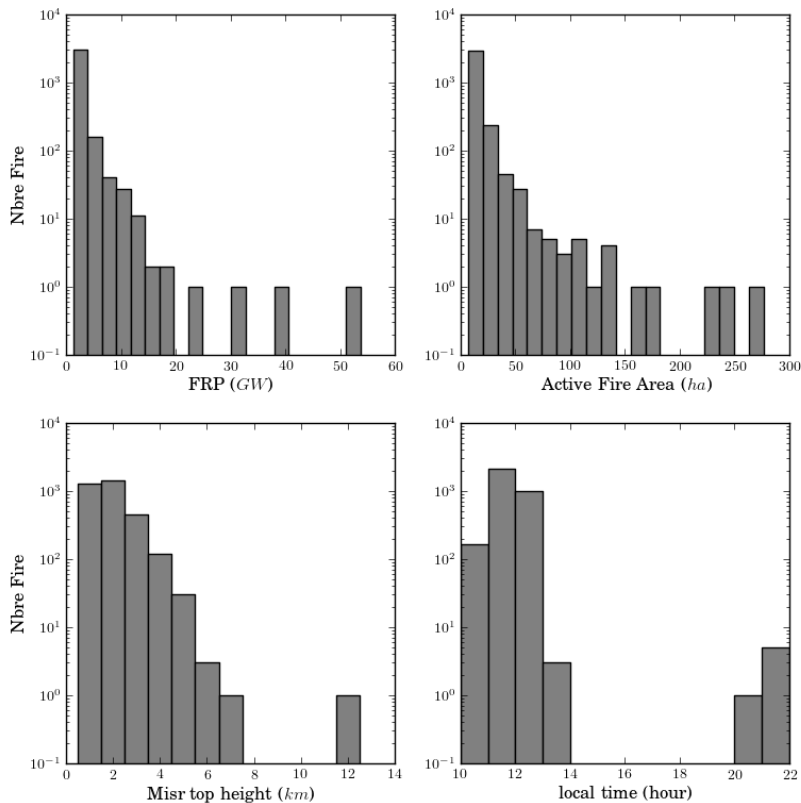
Figure 10. Distribution of FRP, Active fire Area, top plume height, and local time observation time for the 3320 fires of the current North American subset of the Multi-angle Imaging Spectro Radiometer (MISR) plume height project dataset Nelson et al. (2008) derived using the MINX tool shown in Fig. 4.

Figure 11. Overview of the highest fire plumes present in the current North American subset of the MISR plume height dataset of Nelson et al. (2008), derived using the MINX tool shown in Figure 4. The reference of this fire in the MISR data set is O45791-B41-P1, and it was observed in the Northwest Territories (Canada) on 27 July 2008. **(a)** shows the nadir image recorded by MISR, together with the stereo-height retrieval of the MINX model. Part of the image is black as the fire was located on the edge of the MISR swath. **(b)** is the wider-swath Moderate Resolution Imaging Spectroradiometer (MODIS) false color composite image of the area observed at the same time. MODIS is mounted on the same Terra satellite as MISR (see Sect. 4.1). Red pixels denote the location of MODIS pixels detected as containing active fire in the MODIS MOD14 active fire product of (Giglio et al., 2003). Image **(a)** is taken from the MISR plume height project website (see Footnote 1).